



Autoantigen-selected B cells are bystanders in spontaneous T cell-driven experimental autoimmune hepatitis

David Lübbering¹ | Max Preti¹ | Lena Schlott¹ | Christoph Schultheiß²  |
 Sören Weidemann³ | Ansgar W. Lohse¹ | Mascha Binder² |
 Antonella Carambia¹ | Johannes Herkel¹ 

¹First Department of Medicine, University Medical Centre Hamburg-Eppendorf, Hamburg, Germany

²Department of Internal Medicine IV, Oncology/Hematology, Martin-Luther-University Halle-Wittenberg, Halle (Saale), Germany

³Department of Pathology, University Medical Centre Hamburg-Eppendorf, Hamburg, Germany

Correspondence

Antonella Carambia and Johannes Herkel, First Department of Medicine, University Medical Centre Hamburg-Eppendorf, Martinistr. 52, Hamburg 20246, Germany.

Email: a.carambia@uke.de and jherkel@uke.de

Present addresses

Christoph Schultheiß and Mascha Binder, Department of Medical Oncology, Universitätsspital Basel, Basel, Switzerland.

Funding information

Deutsche Forschungsgemeinschaft, Grant/Award Number: SFB 841

Abstract

Autoreactive B cells are considered pathogenic drivers in many autoimmune diseases; however, it is not clear whether autoimmune B cells are invariably pathogenic or whether they can also arise as bystanders of T cell-driven autoimmune pathology. Here, we studied the B cell response in an autoantigen- and CD4⁺ T cell-driven model of autoimmune hepatitis (AIH), the Alb-iGP_Smarta mouse in which expression of a viral model antigen (GP) in hepatocytes and its recognition by GP-specific CD4⁺ T cells causes spontaneous AIH-like disease. T cell-driven AIH in Alb-iGP_Smarta mice was marked by autoantibodies and hepatic infiltration of plasma cells and B cells, particularly of isotype-switched memory B cells, indicating antigen-driven selection and activation. Immunosequencing of B cell receptor repertoires confirmed B cell expansion selectively in the liver, which was most likely driven by the hepatic GP model antigen, as indicated by branched networks of connected sequences and elevated levels of IgG antibodies to GP. However, intrahepatic B cells did not produce increased levels of cytokines and their depletion with anti-CD20 antibody did not alter the CD4⁺ T cell response in Alb-iGP_Smarta mice. Moreover, B cell depletion did not prevent spontaneous liver inflammation and AIH-like disease in Alb-iGP_Smarta mice. In conclusion, selection and isotype-switch of liver-infiltrating B cells was dependent on the presence of CD4⁺ T cells recognizing liver antigen. However, recognition of hepatic antigen by CD4⁺ T cells and CD4⁺ T cell-mediated hepatitis was not dependent on B cells. Thus, autoreactive B cells can be bystanders and need not be drivers of liver inflammation in AIH.

Abbreviations: AIH, autoimmune hepatitis; ALT, alanine aminotransferase; AST, aspartate aminotransferase; BCR, B cell receptor; CDR, complementarity-determining region; GP, glycoprotein; ISW, isotype-switched; mHAI, modified histological activity index; SHM, somatic hypermutation.

David Lübbering and Max Preti should be considered joint first author.

Antonella Carambia and Johannes Herkel should be considered joint senior author.

This is an open access article under the terms of the [Creative Commons Attribution-NonCommercial-NoDerivs](https://creativecommons.org/licenses/by-nc-nd/4.0/) License, which permits use and distribution in any medium, provided the original work is properly cited, the use is non-commercial and no modifications or adaptations are made.

© 2023 The Authors. *Immunology* published by John Wiley & Sons Ltd.

KEYWORDS

autoimmunity, B cell, CD4 cell, liver

INTRODUCTION

Autoimmune diseases are caused by an adaptive immune response to self-antigens; however, their exact pathogenesis is mostly unclear [1, 2]. Autoantibodies are found in many autoimmune diseases, but a direct pathogenic role of autoantibodies is seen only in few conditions, such as in myasthenia gravis or Graves' disease [3]. However, autoreactive B cells can also promote autoimmune diseases by antibody-independent mechanisms: most notable are (1) the secretion of pro-inflammatory cytokines, such as TNF, Interferon- γ or IL-6 [4–6], and (2) the effective collection of autoantigens recognized by the B cell receptor (BCR), which are then presented to activate autoreactive T cells [7–9]. Thus, B cells can be an important pathogenic factor in autoimmune diseases. B cell-depletion therapies, such as by administration of the anti-CD20 antibody Rituximab, have become a promising treatment approach for various autoimmune diseases [10]. However, B cells can also become activated as bystanders during inflammation [11–14], and some B cells can even inhibit autoreactivity, mainly by production of immunosuppressive cytokines, such as IL-10 or IL-35 [15, 16]. Thus, it is possible that B cell-depletion could be ineffective or even disadvantageous in some patients. However, bystander activation of B cells has been mainly described in the context of infection and it is currently not clear to which extent it can occur in autoimmune diseases. Thus, the question is whether autoimmune disease features, such as autoantibodies, or B cell and plasma cell infiltrates within affected organs, could develop by way of bystander activation, or whether these markers invariably indicate B cell-driven pathology.

Here, we analysed the role of B cells in the prototypical CD4⁺ T cell-driven autoimmune disease autoimmune hepatitis (AIH). AIH is a rare, chronic, immune-mediated liver disease characterized by portal hepatic infiltrates and interface hepatitis, accompanied by elevated serum levels of aminotransferases, IgG and autoantibodies [17]. AIH is considered driven by autoreactive T cells recognizing hepatocellular autoantigens, as indicated by predominance of CD4⁺ T cells in lymphocytic liver infiltrates, strong genetic linkage to HLA-DRB1*0301 and HLA-DRB1*0401 haplotypes, and detection of autoantigen-specific CD4⁺ T cells [17, 18]. The known autoantigens, like CYP2D6 and SEPSECS, targeted by anti-LKM1 and anti-SLA/LP autoantibodies respectively, are recognized both by autoreactive B cells and T cells of AIH patients [19–21]. Whereas CD4⁺ T cells predominate in

lymphocytic liver infiltrates of AIH patients, plasma cells and B cells are also present [17, 22], which together with the typical IgG elevation and autoantibodies indicates a possible involvement of B cells in AIH pathogenesis [23]. In type 2 AIH, which is more common in children and young adults, anti-LKM-1 autoantibodies are considered to be directly pathogenic [24]; yet, direct pathogenicity of antibodies has not been shown in type 1 AIH, which is more prevalent in adults. B cell depletion with Rituximab has been tried in small cohorts of difficult-to-treat AIH patients as a third line treatment, albeit under continued immunosuppressive treatment, eliciting biochemical improvement and a reduction of required steroid dosages [25, 26]. Accordingly, in a mouse model of type 2 AIH induced by xenovaccination to human CYP2D6, a single administration of a monoclonal anti-CD20 antibody has been reported to cause histological remission, reduced alanine aminotransferase (ALT) and IgG serum levels, and a decrease in T follicular helper cells [27]. However, in a different AIH mouse model induced by adenoviral immunization to xenogenic human FTCD, no improvements in histological activity and no reduction of transaminase levels were found, but a reduction in serum IgG and an altered serum protein pattern after single-dose administration of anti-CD20 [28]. In yet another AIH model induced by immunization to a mouse liver protein extract, B cell depletion was found to impair regulatory B cells and increase T cell-mediated autoimmunity [29]. Correspondingly, a recent study has shown that mice lacking regulatory B cells develop spontaneous inflammation of several organs, including the liver [30]. Of note, immunosequencing of T cell and BCRs in AIH patients revealed strong skewing in the T cell receptor repertoire, but not in the BCR repertoire, indicating that antigen selection operates mainly in T cells, but not in the B cell compartment [31]. Thus, some findings seem to hint at a pathological role of autoreactive B cells in AIH, whereas others seem compatible with a primarily T cell-driven AIH pathogenesis and a bystander role for B cells in AIH.

To further elucidate the role of B cells in AIH, we took advantage of an autoantigen- and CD4⁺ T cell-driven mouse model of autoimmune liver inflammation, the Alb-iGP_Smarta mice [32]. We consider that model particularly well suited to address this issue because, in contrast to the models detailed above, it develops spontaneously and does not require immunization, which might be a potential confounder. Alb-iGP_Smarta mice feature a liver-restricted model antigen (GP) that is recognized by abundant antigen-specific CD4⁺ T cells. GP-specific T

cell activation in the liver induces spontaneous AIH-like liver inflammation with B cell involvement, as indicated by presence of plasma cells in lymphocytic liver infiltrates, elevated IgG levels and relevant titres of antinuclear autoantibodies. Importantly, antigen-specific CD4⁺ T cells can unambiguously be identified by use of MHC II tetramers loaded with GP peptide. In this study, we characterized hepatic B cell populations in Alb-iGP_Smarta mice via flow cytometry and next-generation immunosequencing. Moreover, we investigated the effect of B cell and plasma cell depletion, using anti-CD20 antibody and bortezomib [33, 34], on autoantigen-specific hepatic CD4⁺ T cells and the clinical course of liver inflammation.

MATERIALS AND METHODS

Animal experimentation

Alb-iGP_Smarta mice were generated as previously described [32]. All mice were bred and maintained under specific pathogen-free conditions at the animal facility of the University Medical Centre Hamburg-Eppendorf (Hamburg, Germany). The mice were monitored daily for sickness symptoms, according to general appearance, body condition, posture, facial expression and mobility for up to 50 weeks. All animals received humane care, and clinical and behavioural humane endpoints were applied to minimize any harm. All animal experiments were conducted in accordance with the Basel Declaration, the European Directive 2010/63/EU, and German federal law. Experiments were approved by the relevant review board and authorities of the State of Hamburg.

Cell isolation and flow cytometry

Mouse livers were perfused in situ with PBS via the portal vein before organ sampling for histology and cell isolation. Lymphocytes from liver and spleen samples were isolated as previously described [32]. In brief, samples were passed through a 100 µm cell strainer and primary liver cells were purified using OptiPrep Density Gradient Medium (Sigma Aldrich) according to the manufacturer's instructions. Red blood cells were removed before staining by ACK Lysing Buffer (ThermoFisher). Single cell suspensions were incubated with Pacific Orange-conjugated succinimidyl ester (ThermoFisher) for dead cell segregation and stained with the following fluorochrome-labelled antibodies: CD45 (clone 30-F11), CD19 (1D3), B220 (RA3-6B2), IgD (11-26c.2a), CD3 (17A2), CD38 (90), CD138 (281-2), CD4 (RM4-5), CD8 (53-6.7), CD25 (PC61), FoxP3 (FJK-16S),

CD44 (IM7), CD62L (MEL-14), I-A^b (AF6-120.1), TNFα (MP6-XT22), IFNγ (XMG1.2), IL-10 (JES5-16E3), IL-17 (TC11-18H10.1) and IL-6 (MP5-20F3) provided by BioLegend as well as IgM (1B4B1; Southern Biotech). APC-conjugated LCMV GP(66-77) I-A^b tetramer was kindly provided by the NIH Tetramer Core Facility. Samples were acquired with a LSRFortessa device (BD Biosciences). The Foxp3/Transcription Factor Staining Buffer Set (ThermoFisher) was used for intracellular staining according to the manufacturer's instructions.

Stimulation assays

For in-vitro CD4⁺ T cell stimulation, primary cells were resuspended in Panserin medium (Pan Biotech) containing 10% foetal bovine serum and 1% penicillin/streptomycin (Gibco) followed by incubation for 5 hours with PMA (50 ng/mL), Ionomycin (1 µg/mL, both Sigma Aldrich) and Brefeldin A (1× GolgiPlug, BD Biosciences). B cells were stimulated in-vitro as previously described [35]. In brief, primary cells were resuspended in complete medium consisting of RPMI 1640 medium (Pan Biotech), 10% foetal bovine serum, 1% penicillin/streptomycin and 5 × 10⁻⁵ M 2-mercaptoethanol (all from Gibco). Subsequently, B cells were incubated for 24 h with LPS (10 µg/mL; Escherichia coli serotype 0111: B4, Sigma-Aldrich) with an agonistic anti-CD40 Ab (10 µg/mL; FGK45, BioLegend) for IL-6 detection. After 19 hours, PMA, ionomycin and Brefeldin A were added in the concentrations mentioned above. Intracellular cytokine staining for flow cytometry was performed as previously described.

B cell and plasma cell depletion

For short-term B cell depletion, 250 µg of anti-CD20 Ab (SA271G2) or rat IgG2b, κ isotype control (RTK4530; BioLegend) were injected intravenously in 6-week-old Alb-iGP_Smarta mice on days 0 and 7. Plasma cell depletion was performed by i.v. administration of bortezomib (0.75 mg/kg, Velcade, Janssen-Cilag) or PBS on days 4.5 and 6. Mice were sacrificed on day 14. The long-term B cell depletion in Alb-iGP_Smarta mice was performed as previously described [34]. In brief, after conducting the B cell and plasma cell depletion treatment as described above for the first 2 weeks, weekly i.v. injections of the anti-CD20 Ab or IgG2b isotype control were maintained for 13 consecutive weeks in total. Long-term treatment was started at the age of 20 weeks. Mouse monitoring for disease symptoms was continued until week 50.

Immunohistochemistry and fluorescence histology

Liver inflammation was visualized via haemalum and eosin (Carl Roth) staining of formalin-fixed, paraffin-embedded mouse liver samples. Samples were analysed by a pathologist in a blinded manner applying the modified histological activity index (mHAI) [36]. B220⁺ B cells and CD4⁺ T cells were stained using the ZytoChem-Plus AP-Polymer-Kit (Zytomed Systems) and the respective antibodies (B220: RA3-6B2, CD4: 4SM95, ThermoFisher). Immunofluorescence staining was performed on acetone-fixed, TissueTek O.C.T. compound (Sakura) embedded liver cryosections with the nuclear dye Hoechst 33258 (ThermoFisher) and directly fluorochrome-labelled antibodies comprising anti-CD4 (RM4-5, BioLegend), anti-B220 (RA3-6B2, BD Biosciences), and anti-Ki-67 (16A8, BioLegend). For quantification of Ki-67, CD4 cell-positive periportal zones were selected using a standardized fluorescence threshold value and Ki-67 mean grey values were then measured in the selected areas using ImageJ Fiji software [37]; the indicated values were calculated as the mean of three representative liver sections per mouse.

Serology

Alanine aminotransferase and aspartate aminotransferase (AST) levels were measured in serum samples using a COBAS Mira System (Roche Diagnostics) at the Institute of Experimental Immunology and Hepatology, University Medical Center Hamburg-Eppendorf. IgG serum levels were analysed using an IgG mouse ELISA Kit (Abcam).

Anti-GP61-80 IgG detection

96-well polystyrene ELISA microplates (Thermo Fisher) were coated overnight with 40 µg/mL recombinant GP61-80 protein (PANATecs). Plates were blocked using 1% bovine serum albumin in 1xPBS. Sera were pre-diluted 1:10 and incubated for 2 h, then IgG detection was performed with reagents from an IgG mouse ELISA kit (Abcam).

Next-generation immunosequencing and data analysis

Isolation of genomic DNA from fresh frozen liver and spleen followed by immunosequencing of B cell repertoires was performed as described in Reference [38]. In

brief, V(D)J rearranged IGH loci were amplified from 500 ng of genomic DNA using a multiplex PCR, pooled at 4 nM and quality-assessed on a 2100 Bioanalyzer (Agilent Technologies). Sequencing was performed on an Illumina MiSeq (paired-end, 2 × 301-cycles, v3 chemistry). Rearranged IGH loci were annotated using MiXCR v3.0.12 [38], and the IMGT v3 IGH library as reference. Non-productive reads and sequences with less than two counts were discarded. Each unique complementarity-determining region 3 (CDR3) was considered as clone. To visualize network connectivity in BCR repertoires, clonal B cell lineages with a Levenshtein distance up to 2 were first assembled using the BRILIA tool [39], and then visualized as petri dish plots with the package igraph and the Fruchterman-Reingold layout [40]. Data analysis and plotting were performed using R version 3.5.1.

Statistical analysis

Statistical analysis was conducted with GraphPad Prism 6 software (GraphPad Software) by using the two-tailed Mann-Whitney U test (two groups), one-way ANOVA and Tukey's multiple comparisons test for normally distributed data, or alternatively, the Kruskal-Wallis test followed by Dunn's test for multiple comparisons (>2 groups). The log-rank (Mantel Cox) test was applied to disease-free survival data. Results in graphs are displayed as mean ± SEM.

RESULTS

Lymphocyte infiltration and increased B cell numbers in early-stage liver inflammation in Alb-iGP_Smarta mice

Liver inflammation in Alb-iGP_Smarta mice can be divided into an asymptomatic early stage in young mice and a subsequent symptomatic stage with spontaneous onset beyond the age of 20 weeks. Early-stage liver inflammation in Alb-iGP_Smarta mice is characterized by portal inflammation and lymphocyte infiltrates in liver histology, whereas Alb-iGP and Smarta control mice do not exhibit hepatitis [32]. In line with these findings, 8-week-old Alb-iGP_Smarta mice show significantly increased numbers of CD45⁺ cells in the liver compared to Alb-iGP and Smarta control mice (Figure 1a). This effect was liver-specific and not detectable in spleen samples (Figure 1a). The percentage of CD19⁺B220⁺ B cells was significantly elevated in the spleen of Alb-iGP_Smarta mice compared to Smarta controls (Figure 1b), but not to Alb-iGP controls, and not in the

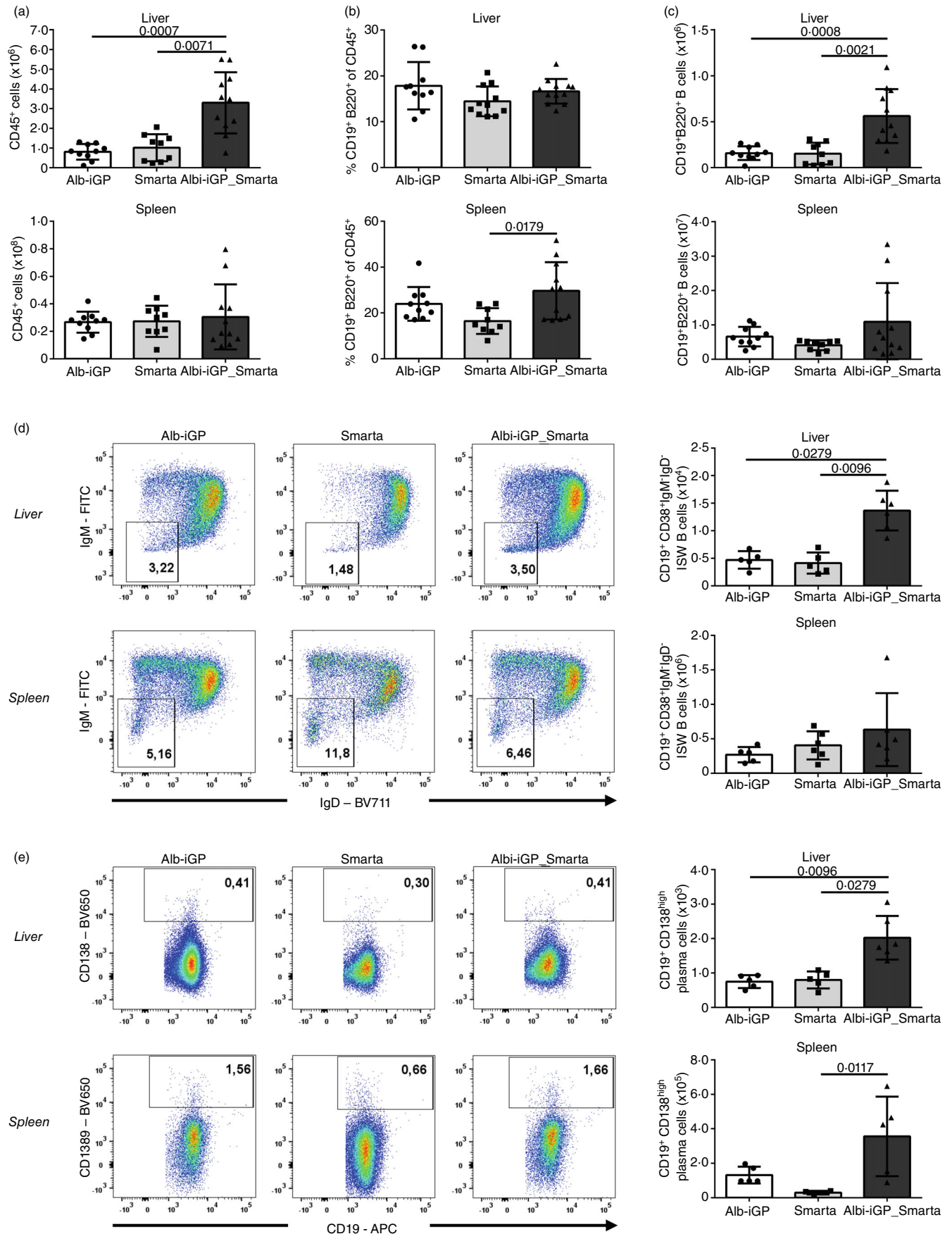


FIGURE 1 Legend on next page.

liver. Accordingly, the total B cell numbers were similar in the spleen of all strains. However, we observed a significant increase in total B cell numbers in the liver of Alb-iGP_Smarta mice as compared to Alb-iGP mice and Smarta mice (Figure 1c). Moreover, we found significantly elevated numbers of CD19⁺CD38⁺IgM⁻IgD⁻ isotype-switched (ISW) memory B cells in the livers of Alb-iGP_Smarta mice (Figure 1d), whereas ISW B cells were not increased in the spleen. Shown are representative flow cytometry plots with frequencies (left), and absolute cell numbers in the bar graphs (right). Furthermore, CD19⁺CD138^{high} plasma cell numbers of Alb-iGP_Smarta mice were significantly increased in the spleen, as compared to Smarta controls (Figure 1e) and in the liver, as compared to both control lines. These findings indicated that CD19⁺B220⁺ B cells infiltrated the livers of Alb-iGP_Smarta mice in early-stage liver inflammation; however they were not expanded relative to other lymphocyte subsets. Nonetheless, the presence of ISW memory B cells and plasma cells in the hepatic infiltrates in Alb-iGP_Smarta mice might indicate an antigenic selection process.

Next-generation immunosequencing demonstrates antigenic selection of hepatic B cells in Alb-iGP_Smarta mice

To address the hypothesis of antigenic selection in the livers of Alb-iGP_Smarta mice, we performed next-generation sequencing for BCR clonotype analysis and profiled global repertoire metrics in liver and spleen. In liver samples, we found a significantly elevated total clone number (richness) in Alb-iGP_Smarta mice compared to samples of Smarta controls (Figure 2a), confirming hepatic B cell infiltration in these mice. In addition, we observed a significantly elevated Shannon index as proxy for increased clonal diversity in the hepatic BCR repertoire of Alb-iGP_Smarta mice compared to Smarta controls (Figure 2a). Moreover, we saw a trend towards a higher rate of IGH somatic hypermutation (SHM) in liver samples of Alb-iGP_Smarta mice, suggesting an elevated number of antigen-experienced memory B cells or plasma

cells in the repertoire (Figure 2a). Interestingly, we did not see similar trends in spleen samples of Alb-iGP_Smarta mice, which did not differ from Smarta controls (Figure 2a). Analysis of the mean clonal space occupied by single clonotypes within the repertoires revealed a selective decrease of the clonal space occupied by hyperexpanded BCR clones, and a corresponding increase of clonotypes that occupy medium and small percentages of clonal space in Alb-iGP_Smarta liver samples (Figure 2b). This differential clonal space architecture was found only in the liver, but not in the spleen (Figure 2b), suggesting antigenic selection in the livers of Alb-iGP_Smarta mice. Accordingly, BCR network analysis revealed an increased connectivity of the BCR repertoire in Alb-iGP_Smarta livers, but not spleens (Figure 2c), confirming the notion of antigen-driven selection in livers of Alb-iGP_Smarta mice. We hypothesized that the antigen driving these repertoire shifts in Alb-iGP_Smarta livers was the GP model autoantigen peptide, as Alb-iGP_Smarta mice are characterized by ectopic expression of the GP peptide in the liver. Indeed, Alb-iGP_Smarta mice with late-stage acute liver inflammation featured significantly elevated IgG antibodies to the GP peptide (Figure 2d). Taken together, the observed BCR repertoire metrics along with a distinct anti-GP antibody response confirmed the notion of GP-driven B cell selection in Alb-iGP_Smarta livers.

B cells do not participate in liver inflammation via enhanced production of pro- or anti-inflammatory cytokines in Alb-iGP_Smarta mice

Having shown antigen-driven B cell selection in the livers of Alb-iGP_Smarta mice, we further investigated whether the expanded hepatic B cells in Alb-iGP_Smarta mice were drivers of early-stage liver inflammation in Alb-iGP_Smarta mice. To address this issue, we stimulated splenic or hepatic B cells in-vitro and assessed the production of cytokines. There was no difference in the production of the pro-inflammatory cytokines TNF (Figure 3a), IFN γ (Figure 3b), and IL-6 (Figure 3c), or the

FIGURE 1 Lymphocyte infiltration and increased B cell numbers in early-stage liver inflammation in Alb-iGP_Smarta mice. (a) CD45⁺ cells in the spleen and liver of Alb-iGP, Smarta and Alb-iGP_Smarta mice. Shown data are pooled from two independent experiments ($n = 7-8$, age 8 weeks). (b) Frequency and (c) count of splenic and hepatic CD19⁺B220⁺ B cells in Alb-iGP, Smarta and Alb-iGP_Smarta mice. Shown data are pooled from two independent experiments ($n = 9-10$, age 8–17 weeks). (d) Representative flow cytometry plots and count of hepatic and splenic CD19⁺CD38⁺IgM⁻IgD⁻ isotype-switched (ISW) B cells and (e) CD19⁺CD138^{high} plasma cells ($n = 5-6$, age 8–17 weeks). Shown data are representative of two independent experiments. Total cell count was calculated per 100 mg of spleen and per gram of liver sample. *P*-values were calculated by Kruskal-Wallis with Dunn's multiple comparisons test, and are indicated only when significant, that is, $p < 0.05$.

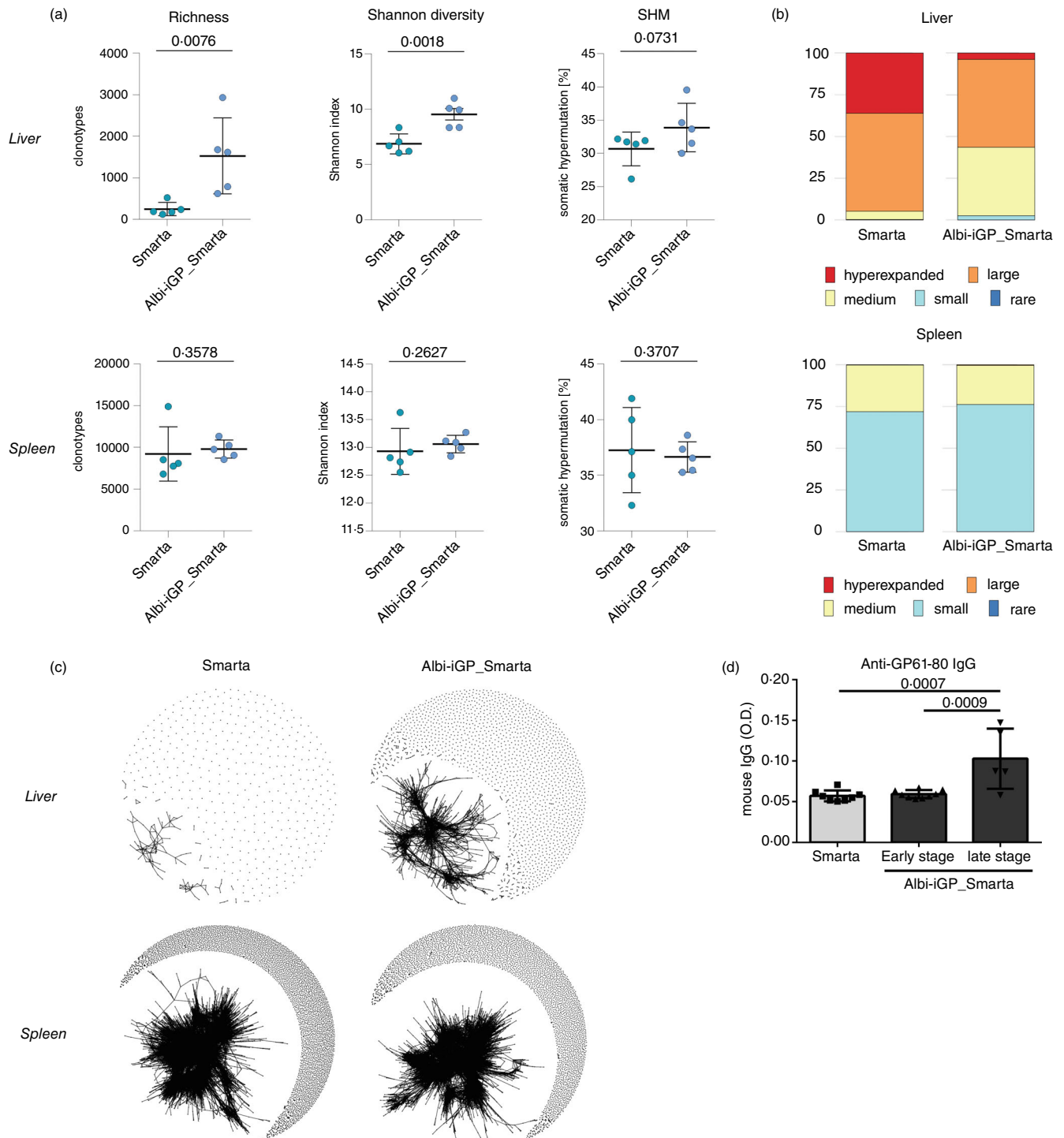


FIGURE 2 Next-generation immunosequencing indicates antigenic selection of hepatic B cells in Alb-iGP_Smarta mice. (a) Mean richness, Shannon diversity index, and somatic hypermutation rate (SHM) for the productive IGH repertoires of liver and spleen samples in 8-week-old Smarta and Alb-iGP_Smarta mice ($n = 5$). (b) Mean distribution of small, medium, large and hyperexpanded clones in % within the clonal B cell space in spleen and liver samples. (c) Network connectivity of BCR repertoires exemplified for one characteristic animal in liver and spleen samples. One node represents one unique CDR3 clonotype independent of frequency. Similar clonotypes (up to Levenshtein distance of 2) are connected by edges. (d) Anti-GP antibodies measured by ELISA in 8-week-old Smarta and Alb-iGP_Smarta mice, along with Alb-iGP_Smarta mice showing symptoms of late-stage liver inflammation ($n = 5-9$). P -values were calculated by Mann-Whitney, or ANOVA with Tukey's multiple comparisons tests.

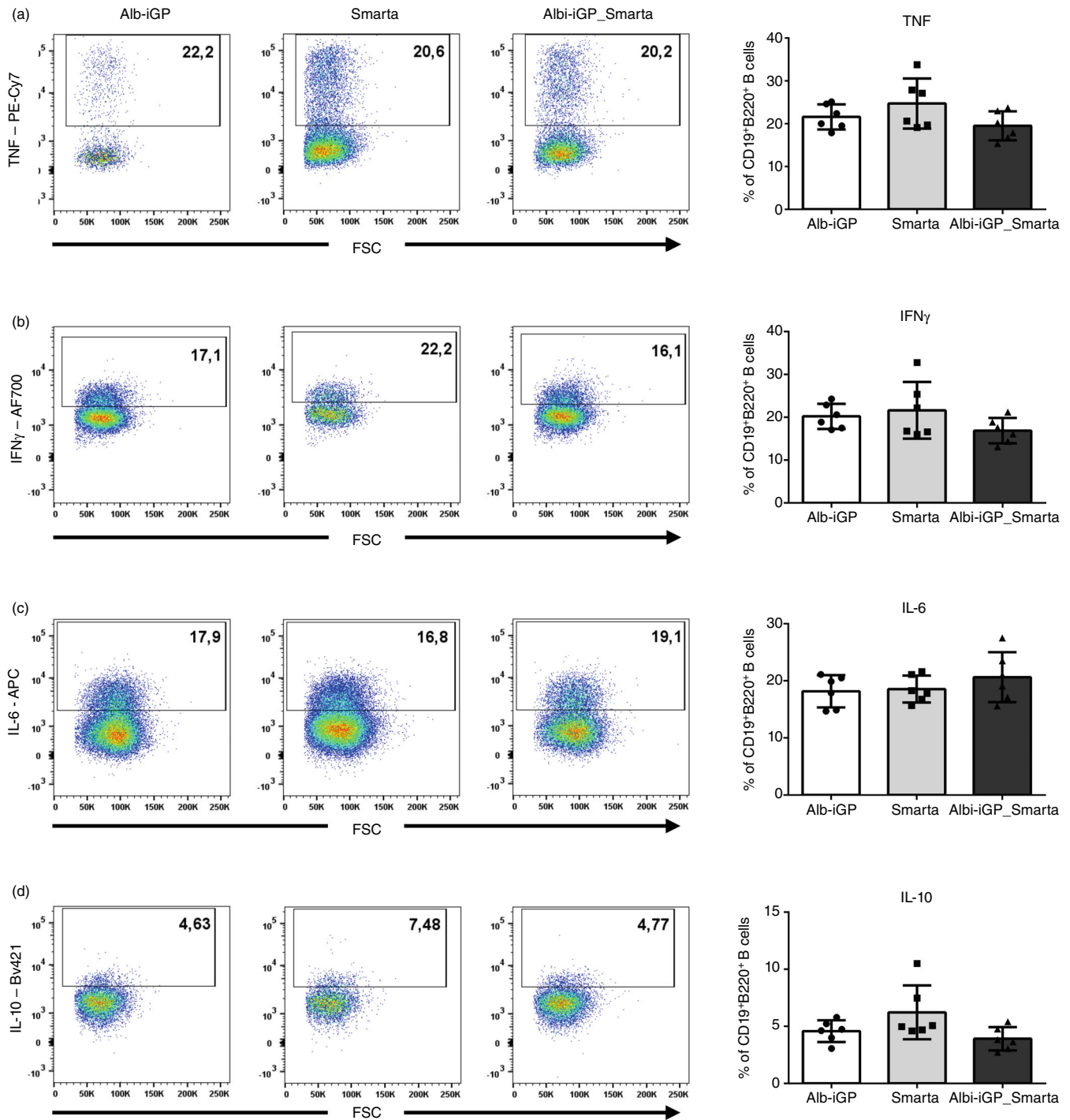


FIGURE 3 Cytokine production by hepatic B cells in early-stage liver inflammation of Alb-iGP_Smarta mice. In-vitro restimulation of hepatic CD19⁺B220⁺ B cells for 24 h with LPS (*Escherichia coli*, O111:B4). An anti-CD40 antibody (FDK45) was added for IL-6 detection. PMA, Ionomycin and Brefeldin A were added for the last 5 h of stimulation. Representative flow cytometry plots and frequencies of (a) TNF, (b) IFN γ , (c) IL-6 and (d) IL-10 producing hepatic B cells in Alb-iGP, Smarta and Alb-iGP_Smarta mice ($n = 6$, age 12–19 weeks). P -values were calculated by Kruskal-Wallis with Dunn's multiple comparisons test, and are indicated only when significant, that is, $p < 0.05$.

anti-inflammatory cytokine IL-10 (Figure 3d) in B cells from Alb-iGP_Smarta livers, as compared to Alb-iGP and Smarta control B cells. Correspondingly, there was no difference in cytokine production in splenic B cells between Alb-iGP_Smarta and Alb-iGP and Smarta control mice

(Supplementary Figure 1A–D). Moreover, the mean fluorescence intensity of the cytokines did not significantly differ between the groups, neither in the liver (Supplementary Figure 2A) nor the spleen (Supplementary Figure 2B), except for higher IFN γ and IL-10 fluorescence in B cells

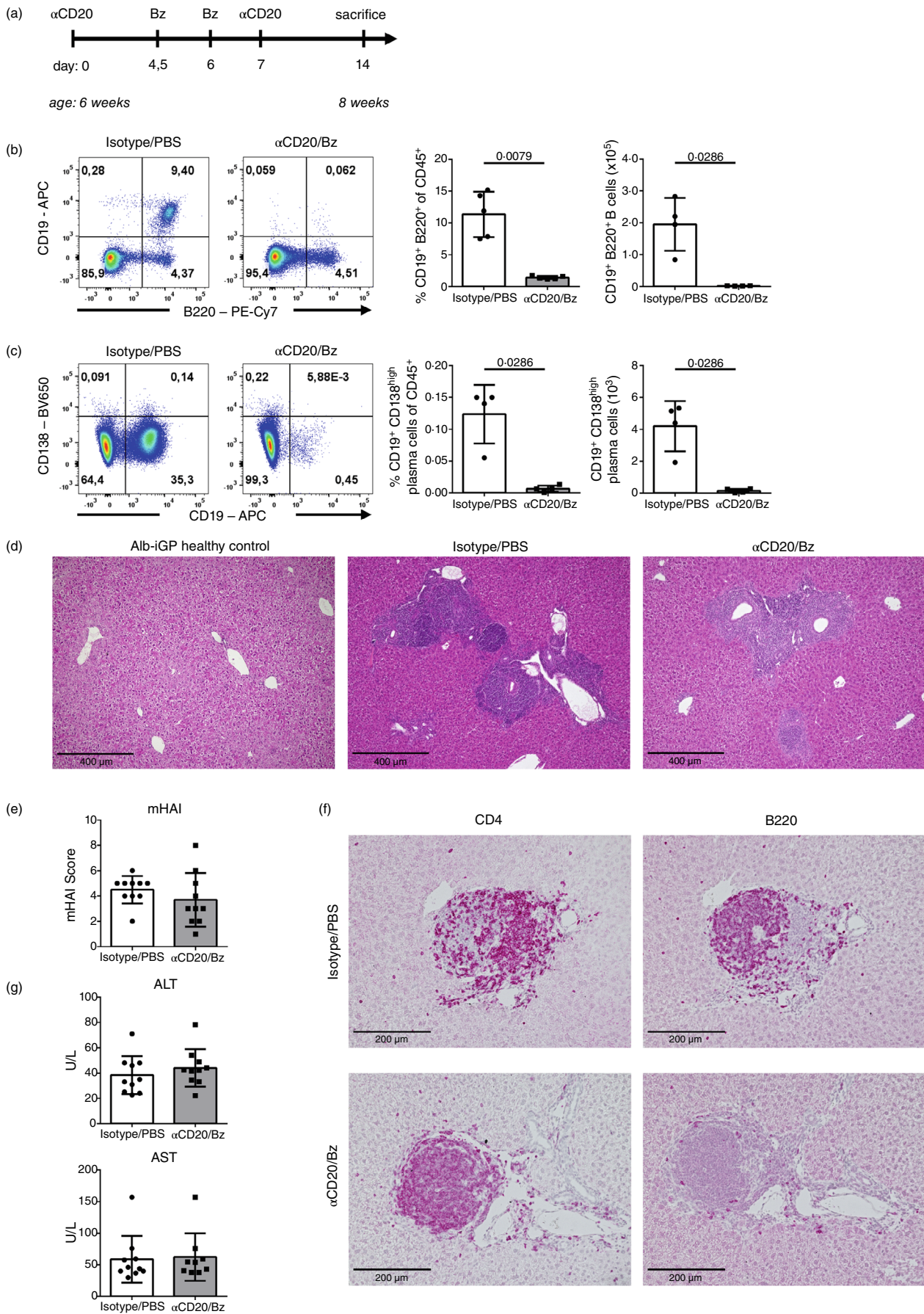


FIGURE 4 Legend on next page.

from Smarta control mice. These findings indicated that B cells in Alb-iGP_Smarta mice did not contribute to liver inflammation by enhanced production of pro-inflammatory cytokines.

In-vivo B cell and plasma cell depletion via a CD20 neutralizing antibody and bortezomib does not alter key characteristics of early-stage liver disease

To uncover a possible contribution of B cells to liver inflammation in Alb-iGP_Smarta mice, we performed a short-term B cell and plasma cell depletion experiment using a monoclonal anti-CD20 antibody and the proteasome inhibitor Bortezomib in 6-week-old Alb-iGP_Smarta mice. To that end, mice were injected intravenously twice with 250 µg of anti-CD20 antibody at days 0 and 7 and twice with Bortezomib with 0.75 mg/kg at days 4.5 and 6 (Figure 4a). As control, Alb-iGP_Smarta mice were injected with 250 µg of non-specific, isotype-matched rat IgG2b antibodies and PBS, respectively. The depletion protocol led to a 99.29% reduction of hepatic CD19⁺B220⁺ B cells (Figure 4b; mean B cell count 1.95×10^5 vs. 1.38×10^3) and a 92.96% reduction of hepatic CD19⁺CD138^{high} plasma cells (Figure 4c; mean plasma cell count 795 vs. 56) compared to controls. B cells and plasma cells were also significantly depleted in the spleen (Supplementary Figure 3). We then investigated whether B cell depletion had an effect on key features of early-stage liver disease in Alb-iGP_Smarta mice and found that portal inflammation was still present in B cell and plasma cell depleted mice, as well as in controls (Figure 4d); for comparison, liver histology of a healthy liver from an Alb-iGP control mouse lacking periportal infiltrates is also shown. Correspondingly, histological activity scored by a pathologist in a blinded manner using

the modified histologic activity index (mHAI) indicated moderate histological activity that was not significantly changed by depletion of B cells and plasma cells (Figure 4e). Immunohistochemistry of liver samples demonstrated that CD4⁺ T cells persisted in periportal infiltrates of B cell and plasma cell depleted mice, whereas B220⁺ B cells were virtually absent (Figure 4f). There were no significant differences in ALT (Figure 4g) or AST (Figure 4g) levels, which, as expected in this early disease stage, were low, both in B cell and plasma cell depleted mice and non-depleted controls.

We then analysed the effect of B cell depletion on frequency and phenotype of the hepatic T cells. We found no significant change in overall hepatic CD4⁺ T cell numbers (Figure 5a, left) in B cell and plasma cell depleted Alb-iGP_Smarta mice. Of note, there was also no difference in the numbers of hepatic GP-specific CD4⁺ T cells (Figure 5a, right), detected by using I-A (b) LCMV GP 66-77 tetramers. Moreover, the numbers of hepatic CD8⁺ T cells were not changed by B cell depletion (Figure 5b). Furthermore, the frequencies of overall (Figure 5c, left) and GP-reactive (Figure 5c, right) CD4⁺CD44^{high}CD62L^{low} Effector Memory (EM) T cells, as well as overall (Figure 5d, left) and GP-specific (Figure 5d, right) CD4⁺CD25⁺FoxP3⁺ regulatory T cells were unchanged in B cell and plasma cell depleted mice, as compared to controls. Cytokine production by CD4⁺ T cells, in particular TNF and IFN γ , is another key characteristic of early-stage liver inflammation in Alb-iGP_Smarta mice [32]; however, the production of TNF, IFN γ , IL-10 and IL-17 by CD4⁺ T cells was not significantly altered in B cell and plasma cell depleted, compared to control mice (Figure 5e). Moreover, the mean fluorescence intensities of these cytokines were not significantly changed by B cell depletion (Supplementary Figure 3E). As CD4⁺ T cells were still present in periportal infiltrates in B cell and plasma cell depleted

FIGURE 4 Short-term B cell and plasma cell depletion via a CD20 neutralizing antibody and Bortezomib does not alter key characteristics of early-stage liver disease in Alb-iGP_Smarta mice. (a) Experimental setup of B cell and plasma cell depletion in 6-week-old Alb-iGP_Smarta mice via intravenous injection of a CD20 neutralizing antibody (Biolegend, SA271G2) and Bortezomib (Janssen-Cilag, Velcade®). Control mice received a rat IgG2b isotype control (Biolegend, RTK4530) and PBS. (b) Representative flow cytometry plots, frequency of CD19⁺B220⁺ B cells of CD45⁺ cells and total cell count of CD19⁺B220⁺ B cells in liver samples of B cell/plasma-cell depleted Alb-iGP_Smarta mice and controls ($n = 5$). (c) Representative flow cytometry plots, frequency of CD19⁺CD138^{high} plasma cells of CD45⁺ cells and total cell count of CD19⁺CD138^{high} plasma cells in liver samples of B cell/plasma cell-depleted Alb-iGP_Smarta mice and controls ($n = 5$). Total cell count was calculated per 100 mg of spleen and per gram of liver sample; shown data are representative of two independent experiments (b, c). (d) Representative H&E liver histology of a healthy Alb-iGP control mouse (left), in comparison to B cell/plasma cell-depleted (right) as well as isotype/PBS-treated (middle) Alb-iGP_Smarta mice. Both, B cell/plasma cell-depleted and control Alb-iGP_Smarta mice are marked by extensive periportal infiltrates. (e) Histological activity assessed by the mHAI score of B cell/plasma cell depleted Alb-iGP Smarta mice and controls ($n = 10$ per group). (f) Representative immunohistochemistry staining of CD4 and B220 in periportal infiltrates in livers of B cell/plasma cell-depleted Alb-iGP_Smarta mice and controls. (g) Serum ALT and AST levels in B cell/plasma cell-depleted Alb-iGP_Smarta mice and controls. ($n = 9-10$ per group). Data are pooled from two independent experiments (e, g). *P*-values were calculated by the Mann-Whitney test, and are indicated only when significant, that is, $p < 0.05$.

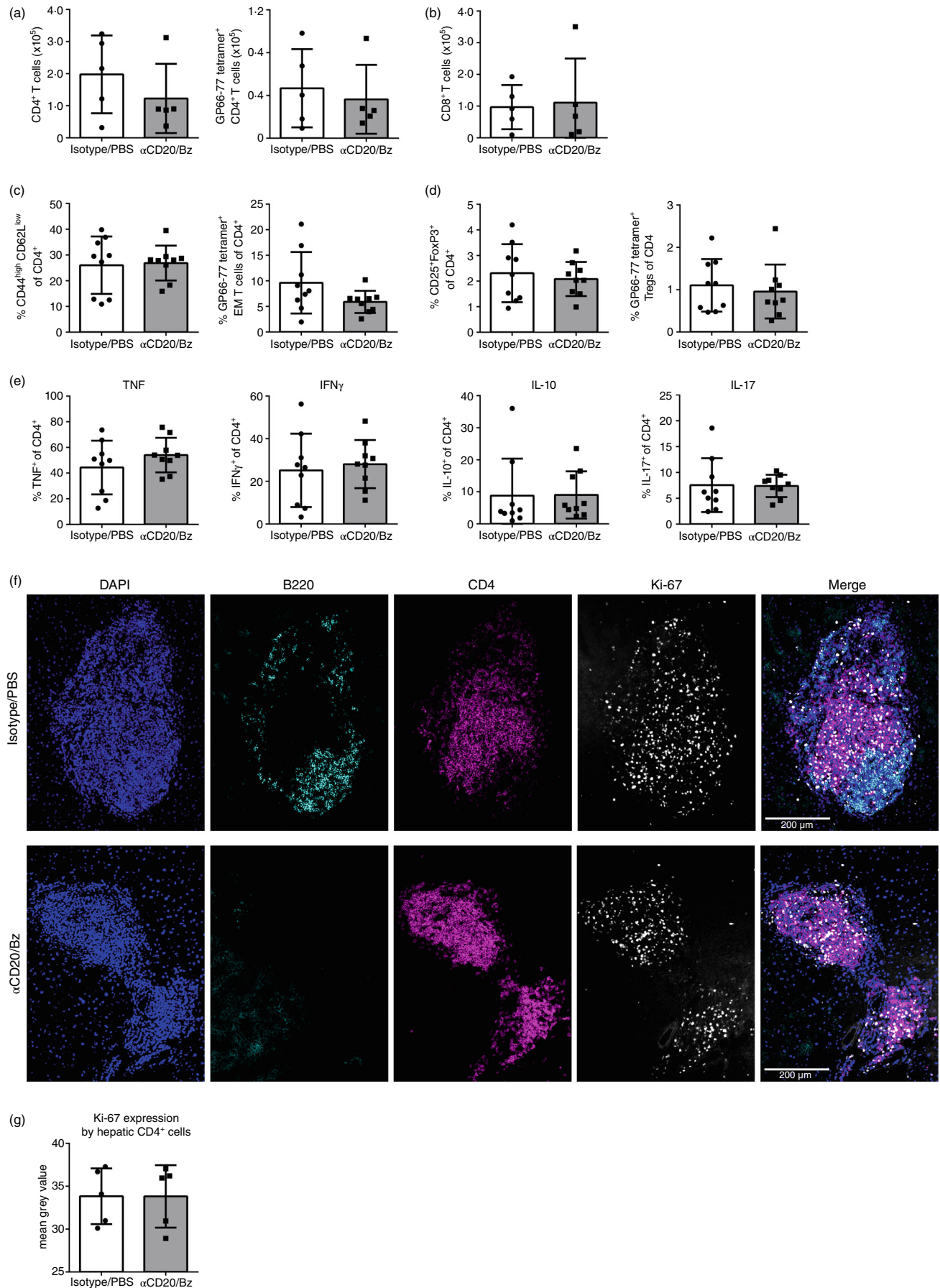


FIGURE 5 Legend on next page.

Alb-iGP_Smarta mice, we investigated whether these cells still proliferated within the inflamed livers. Therefore, we used 4-colour immunofluorescence to visualize B cells and T cells in portal lymphocytic infiltrates. Although B cells were effectively depleted, as indicated by B220 staining, the remaining CD4⁺ T cells in the periportal infiltrates continued to proliferate locally, as indicated by a similar degree of Ki-67 expression in hepatic CD4⁺ T cell zones of B cell and plasma cell depleted or control mice (Figure 5f); Ki-67 quantification, normalized to CD4, is shown in Figure 5g. These findings demonstrated that B cell and plasma cell depletion did not affect key disease features of early-stage liver inflammation, nor did it change the phenotype, activation or local proliferation of hepatic CD4⁺ T cells in Alb-iGP_Smarta mice.

Long-term B cell and plasma cell depletion does not prevent the onset of late-stage liver inflammation in Alb-iGP_Smarta mice

As B cell depletion did not change early disease features in Alb-iGP_Smarta mice, we then determined the effect of B cell depletion on late-stage liver inflammation in Alb-iGP_Smarta mice. To that end, we maintained depletion by weekly injections of anti-CD20 antibody starting at the age of 20 weeks over a course of 13 weeks; in addition, two injections of bortezomib were given in the first week as indicated in the scheme in Figure 6a. Mice were then monitored until the age of 50 weeks and animals showing sickness symptoms of late-stage liver inflammation (described before in [32]) were analysed. Depletion of CD19⁺B220⁺ B cells was effective throughout the observation period, both in the spleen and the liver (Figure 6b); however, the initial injections of bortezomib could not maintain significantly decreased numbers of CD19⁺CD138^{high} plasma cells throughout the entire

experiment in the spleen and liver (Figure 6c), although there was still a trend towards decreased plasma cell numbers in the liver ($P = 0.0667$). Importantly, we observed no significant difference in the incidence and time of onset of late-stage liver inflammation and thus no effect of B cell and plasma cell depletion on the symptom-free survival of Alb-iGP_Smarta mice (Figure 6d). In addition, key characteristics of late-stage liver inflammation, including elevated ALT and AST levels (Figure 6e), as well as the numbers of liver-infiltrating CD4⁺ T cells (Figure 6f), GP-specific CD4⁺ T cells and CD8⁺ T cells (Figure 6g) were not altered. Correspondingly, both B cell and plasma cell depleted mice and isotype and PBS treated controls manifested portal inflammation and interface hepatitis in H&E liver sections, and a similarly high degree of histological activity, as scored by a pathologist using the mHAI score (Figure 6h). These findings indicated that B cells are not required for the onset and perpetuation of late-stage liver inflammation; hence, B cells are bystanders, rather than drivers of liver inflammation in Alb-iGP_Smarta mice.

DISCUSSION

Human AIH is associated with an autoimmune B cell response, as indicated by the presence of autoantibodies, IgG elevation and hepatic infiltration of B cells and plasma cells. It is therefore conceivable that autoreactive B cells might contribute to AIH pathogenesis, either directly, that is, through liver-damaging autoantibodies, or indirectly by modulating autoreactive T cell responses, that is, through the secretion of pro-inflammatory cytokines like TNF or IL-6 [4], or through effective presentation of autoantigen to CD4⁺ T cells via MHC class II [7, 8]. This notion is supported by the finding that known AIH autoantigens, such as Cyp2D6 or SepSecS, are recognized both by autoreactive B cells and T cells of AIH

FIGURE 5 Short-term B cell and plasma cell depletion does not change hepatic CD4⁺ T cell numbers, activation and local proliferation. (a) Hepatic CD4⁺ T cell count (left), LCMV GP66-77 I-A^b tetramer⁺ CD4⁺ T cell count and (b) CD8⁺ T cell count in B cell/plasma cell depleted Alb-iGP_Smarta mice and controls ($n = 5$ per group). Total cell count was calculated per 100 mg of spleen and per gram of liver sample; shown data are representative of two independent experiments (a, b). (c) Frequency of hepatic CD4⁺CD44^{high}CD62L^{low} effector memory (EM) T cells, LCMV GP66-77 I-A^b tetramer⁺ EM CD4⁺ T cells and (d) CD4⁺CD25⁺FoxP3⁺ regulatory T cells (Tregs) and LCMV GP66-77 I-A^b tetramer⁺ Tregs in B cell/plasma cell depleted Alb-iGP_Smarta mice and controls ($n = 9-10$). (e) TNF, IFN γ , IL-10 and IL-17 production by hepatic CD4⁺ T cells after in-vitro restimulation with PMA, Ionomycin and Brefeldin A for 5 h ($n = 9-10$). Shown data are pooled from two independent experiments (c-e). (f) Representative direct immunofluorescence staining of B220 (cyan), CD4 (magenta), and Ki-67 (grey) in liver samples of B cell/plasma cell-depleted Alb-iGP_Smarta mice and controls. Nuclei are stained in blue. (g) Ki-67 mean grey values of three periportal CD4⁺ zones per mouse in B cell/plasma cell depleted or isotype/PBS-treated Alb-iGP_Smarta mice ($n = 5$ per group). P -values were calculated by the Mann-Whitney test, and are indicated only when significant, that is, $p < 0.05$.

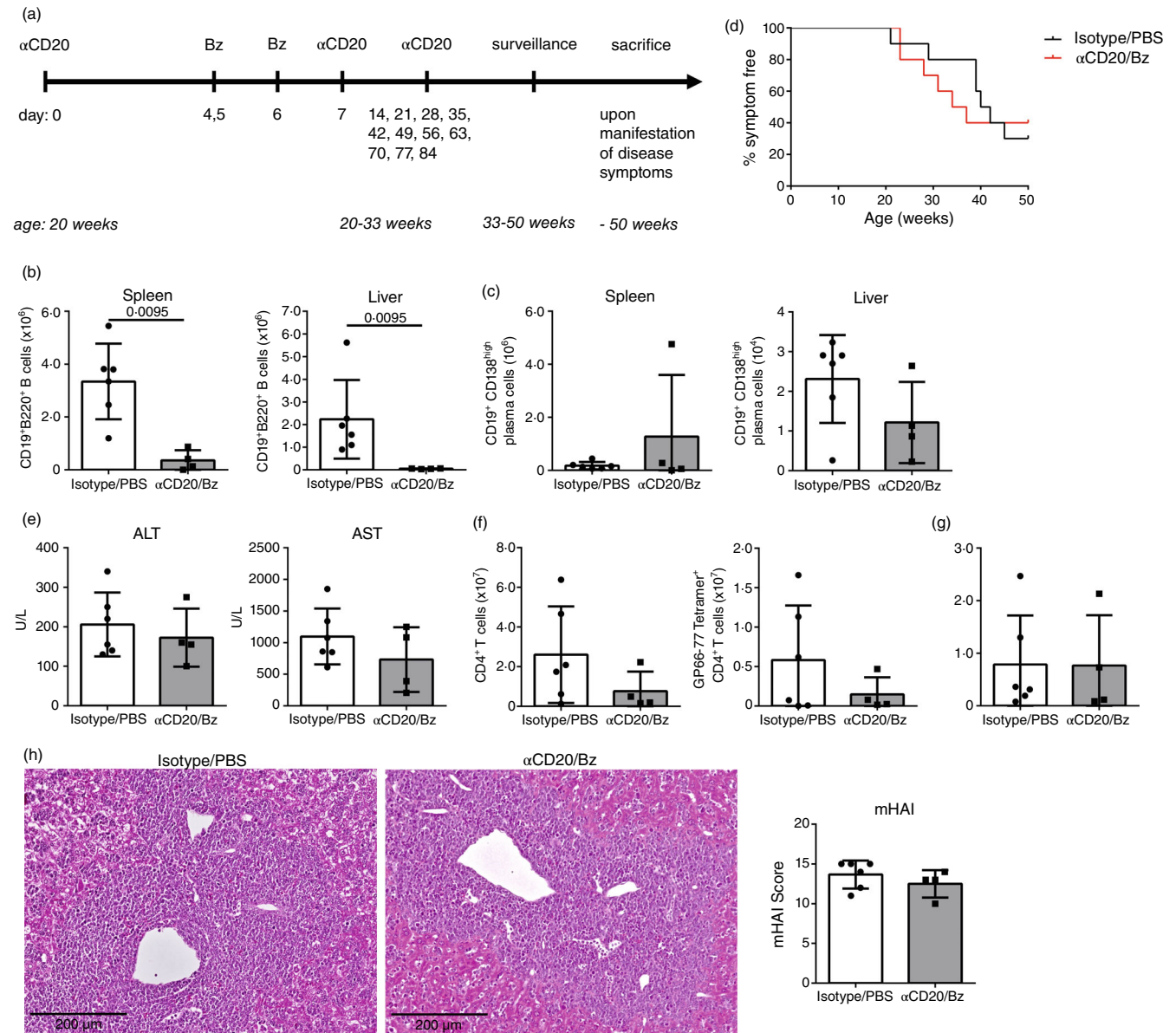


FIGURE 6 Long-term B cell and plasma cell depletion does not prevent the onset of late-stage liver inflammation in Alb-iGP_Smarta mice. (a) Experimental setup of B cell and plasma cell depletion starting in advanced stage at the age of 20 weeks, as indicated; the weekly anti-CD20 injections were continued for 13 weeks. (b) Total count of CD19⁺B220⁺ B cells and (c) CD19⁺CD138^{high} plasma cells in B cell/plasma cell depleted and control Alb-iGP_Smarta mice with symptoms of late-stage liver inflammation ($n = 4-6$ per group). (d) Spontaneous development of sickness symptoms, shown as age-dependent reduced percentage of symptom-free Alb-iGP_Smarta mice under B cell/plasma cell depletion or isotype/PBS injections ($n = 10$ per group). (e) Serum ALT and AST levels in sick B cell/plasma cell depleted and control Alb-iGP_Smarta mice with symptoms of late-stage liver inflammation ($n = 4-5$ per group). (f) Hepatic CD4⁺ T cell count, LCMV GP66-77 I-A^b tetramer⁺ CD4⁺ T cell count and (g) CD8⁺ T cell count in B cell/plasma cell depleted Alb-iGP_Smarta mice and controls ($n = 4-5$ per group). (h) Representative H&E histology showing portal inflammation and interface hepatitis, and mHAI score of B cell/plasma cell depleted and control Alb-iGP_Smarta mice with symptoms of late-stage liver disease ($n = 4-6$). Total cell count was calculated per 100 mg of spleen and per gram of liver sample. P -values were calculated by the Mantel-Cox-test (d) or the Mann-Whitney test, and are indicated only when significant, that is, $p < 0.05$.

patients [19–21]. However, it is likewise possible that the autoreactive B cell response in AIH is non-pathogenic, and develops as a side-effect of a self-damaging T cell response through bystander activation. That notion is supported by the finding that the T cell receptor repertoires of

AIH patients are profoundly skewed, whereas the BCR repertoires of AIH patients are only slightly skewed [31]. Moreover, T cell-derived B cell-activating cytokines, such as IL-21, can be increased in AIH patients, promoting non-specific B cell pro-inflammatory activities [41, 42].

As the exact role of B cells is difficult to address in humans, we have here investigated this issue in Alb-iGP_Smarta mice in which a liver-restricted model antigen is recognized by antigen-specific CD4⁺ T cells, leading to spontaneous autoimmune liver inflammation [32]. Similar to human AIH, these mice display signs of B cell involvement, including the presence of plasma cells in lymphocytic liver infiltrates, elevated IgG levels and relevant titres of antinuclear autoantibodies [32]. Here, we found that the liver infiltrates of Alb-iGP_Smarta mice comprised not only plasma cells, but also elevated numbers of B cells (Figure 1), as has been shown in human AIH [17, 22]. Moreover, we found elevated numbers of isotype-switched memory B cells in the hepatic infiltrates of Alb-iGP_Smarta mice, indicating antigenic selection. Next-generation immunosequencing confirmed liver-specific B cell networks in Alb-iGP_Smarta mice that suggest antigenic selection, which was compatible with the elevated anti-GP antibodies in Alb-iGP_Smarta mice (Figure 2). These findings indicated that the GP antigen was recognized both by B cells and T cells, as has been found in human AIH. Thus, this finding seemed to support the notion that GP-specific B cells might activate GP-specific T cells either by cytokines or GP-presentation. However, we did not detect increased cytokine production by hepatic B cells in Alb-iGP_Smarta mice (Figure 3), and, more importantly, B cell depletion did not alter the T cell response of these mice, and particularly not the response of the GP-specific CD4⁺ T cells (Figure 4, Figure 5). Moreover, even sustained B cell depletion over several weeks did not change the incidence and course of CD4⁺ T cell-driven hepatitis and AIH-like disease (Figure 6). These findings clearly demonstrated that B cells were dispensable for T cell-driven AIH in mice.

The question is to what extent the findings in the mouse model can be translated to human AIH. The mouse model showed B cell metrics compatible with antigenic selection in the liver (Figure 2), although it is evident that liver-inflammation in these mice is primarily CD4⁺ T cell-driven [32]. Thus, an autoreactive B cell response to a liver antigen can develop secondary to a primary autoreactive T cell response to hepatic antigen. In accordance with our findings in the mouse model, a prominent skewing of T cell receptor repertoires, but only slight skewing of BCR repertoires has been reported in human AIH livers [31], possibly indicating that the B cell response in human AIH might also be secondary to a primary autoreactive T cell response. Moreover, the mouse model showed an increase in absolute B cell numbers in the liver; yet there was no selective increase of B cells among the CD45⁺ cells, suggesting non-selective B cell recruitment into the inflamed liver (Figure 1). Thus, the

elevated B cell numbers found in human AIH [17, 22] are not necessarily positive evidence of B cell-driven pathogenesis, but could also be compatible with bystander activation of autoreactive B cells in the course of T cell-driven autoimmune liver inflammation.

Like some autoantigens in human AIH, the GP model antigen in the mouse was recognized both by GP-specific T cells and specific B cells, indicated by presence of IgG antibodies to GP. Yet the continued activation of autoreactive CD4⁺ T cells did not depend on autoantigen presentation by B cells, as it was unaffected by B cell depletion. This finding confirmed that autoreactive B cells were dispensable as antigen-presenting cells for the pathogenic T cell response. It is thus likely that T cell activation was maintained by other antigen presenting cells, most notably dendritic cells, which are elevated in livers of Alb-iGP_Smarta mice and also in AIH patients [32, 43, 44]. However, our findings do not rule out the possibility that antigen-presenting B cells were relevant in the initiation of autoimmune pathogenesis. Indeed, it has been shown that antigen presentation by B cells is particularly relevant in case of low antigen doses [45]. Be that as it may, our findings indicate that maintenance of T cell activation and disease activity might not depend on B cells, and other antigen presenting cells might compensate for B cell depletion. It remains to be seen whether B cell-targeted treatments are effective in human AIH. Preliminary findings indicate at least some efficacy of B cell depleting treatment in AIH patients [25, 26]. More extensive experience in other autoimmune diseases, notably those with a more definite pathogenic role of B cells or autoantibodies, such as lupus or rheumatoid diseases, indicates that B cell-targeted therapies are effective in some patients, while being ineffective or even detrimental in other patients [46, 47]. It is conceivable that individual autoantigen doses might be a relevant determinant here [45], as these may limit the extent to which non-B cells might compensate for the loss of antigen presentation by B cells following their depletion. In the studied mouse model, antigen dose obviously was not a limitation for effective T cell stimulation independent of B cells, but it remains to be seen whether individual AIH patients will respond differently to B cell depletion therapy. Either way, our findings indicate that the presence of autoreactive B cells and autoantibodies as such is not a predictor of the response to B cell depletion therapy.

Taken together, our findings demonstrate that whereas selection of B cells recognizing hepatic antigen required T cell help by antigen-specific CD4⁺ T cells, conversely, activation of autoreactive CD4⁺ T cells and maintenance of liver inflammation was B cell-independent. Our study suggests that autoantibodies and organ-infiltrating B and plasma cells are not a reliable indicator



of B cell-driven autoimmune pathogenesis, because these features can also develop by way of bystander activation.

AUTHOR CONTRIBUTIONS

Acquisition, analysis or interpretation of data for the work: David Lübbering, Max Preti, Lena Schlott, Christoph Schultheiß, Sören Weidemann. Conception or design of the work: David Lübbering, Max Preti, Ansgar W. Lohse, Mascha Binder, Antonella Carambia, Johannes Herkel. Drafting or revising, and approving the manuscript: all authors. Acceptance of accountability for all aspects of the work: all authors.

ACKNOWLEDGEMENTS

We are grateful for excellent technical assistance by Marko Hilken, Sabrina Kress, Gela Schmidt and Jenny Wigger. Open Access funding enabled and organized by Projekt DEAL.

CONFLICT OF INTEREST STATEMENT

The authors declare no conflicts of interest.

DATA AVAILABILITY STATEMENT

The data that support the findings of this study are available from the corresponding author upon reasonable request.

ORCID

Christoph Schultheiß  <https://orcid.org/0000-0001-9789-5776>

Johannes Herkel  <https://orcid.org/0000-0001-9055-9999>

REFERENCES

- Davidson A, Diamond B. Autoimmune diseases. *N Engl J Med*. 2001;345:340–50.
- Theofilopoulos AN, Kono DH, Baccala R. The multiple pathways to autoimmunity. *Nat Immunol*. 2017;18:716–24.
- Ludwig RJ, Vanhoorelbeke K, Leyboldt F, Kaya Z, Bieber K, McLachlan SM, et al. Mechanisms of autoantibody-induced pathology. *Front Immunol*. 2017;8:603.
- Shen P, Fillatreau S. Antibody-independent functions of B cells: a focus on cytokines. *Nat Rev Immunol*. 2015;15:441–51.
- Cyster JG, Allen CDC. B cell responses: cell interaction dynamics and decisions. *Cell*. 2019;177:524–40.
- Barr TA, Shen P, Brown S, Lampropoulou V, Roch T, Lawrie S, et al. B cell depletion therapy ameliorates autoimmune disease through ablation of IL-6-producing B cells. *J Exp Med*. 2012;209:1001–10.
- O'Neill SK, Shlomchik MJ, Glant TT, Cao Y, Doodes PD, Finnegan A. Antigen-specific B cells are required as APCs and autoantibody-producing cells for induction of severe autoimmune arthritis. *J Immunol*. 2005;174:3781–8.
- Serreze DV, Fleming SA, Chapman HD, Richard SD, Leiter EH, Tisch RM. B lymphocytes are critical antigen-presenting cells for the initiation of T cell-mediated autoimmune diabetes in nonobese diabetic mice. *J Immunol*. 1998;161:3912–8.
- Molnarfi N, Schulze-Topphoff U, Weber MS, Patarroyo JC, Prod'homme T, Varrin-Doyer M, et al. MHC class II-dependent B cell APC function is required for induction of CNS autoimmunity independent of myelin-specific antibodies. *J Exp Med*. 2013;210:2921–37.
- Casan JML, Wong J, Northcott MJ, Opat S. Anti-CD20 monoclonal antibodies: reviewing a revolution. *Hum Vaccin Immunother*. 2018;14:2820–41.
- Jiang W, Johnson D, Adekunle R, Heather H, Xu W, Cong X, et al. COVID-19 is associated with bystander polyclonal autoreactive B cell activation as reflected by a broad autoantibody production, but none is linked to disease severity. *J Med Virol*. 2023;95:e28134.
- Chung JB, Wells AD, Adler S, Jacob A, Turka LA, Monroe JG. Incomplete activation of CD4 T cells by antigen-presenting transitional immature B cells: implications for peripheral B and T cell responsiveness. *J Immunol*. 2003;171:1758–67.
- Sanderson NS, Zimmermann M, Eilinger L, Gubser C, Schaeren-Wiemers N, Lindberg RL, et al. Cocapture of cognate and bystander antigens can activate autoreactive B cells. *Proc Natl Acad Sci USA*. 2017;114:734–9.
- Gardell JL, Parker DC. CD40L is transferred to antigen-presenting B cells during delivery of T-cell help. *Eur J Immunol*. 2017;47:41–50.
- Shalpour S, Lin XJ, Bastian IN, Brain J, Burt AD, Aksenov AA, et al. Inflammation-induced IgA+ cells dismantle anti-liver cancer immunity. *Nature*. 2017;551:340–5.
- Rosser EC, Mauri C. Regulatory B cells: origin, phenotype, and function. *Immunity*. 2015;42:607–12.
- Mieli-Vergani G, Vergani D, Czaja AJ, Manns MP, Krawitt EL, Vierling JM, et al. Autoimmune hepatitis. *Nat Rev Dis Primers*. 2018;4:18017.
- Herkel J, Carambia A, Lohse AW. Autoimmune hepatitis: possible triggers, potential treatments. *J Hepatol*. 2020;73:446–8.
- Löhr HF, Schlaak JF, Lohse AW, Böcher WO, Arenz M, Gerken G, et al. Autoreactive CD4+ LKM-specific and anticlonotypic T-cell responses in LKM-1 antibody-positive autoimmune hepatitis. *Hepatology*. 1996;24:1416–21.
- Ma Y, Bogdanos DP, Hussain MJ, Underhill J, Bansal S, Longhi MS, et al. Polyclonal T-cell responses to cytochrome P450IID6 are associated with disease activity in autoimmune hepatitis type 2. *Gastroenterology*. 2006;130:868–82.
- Mix H, Weiler-Normann C, Thimme R, Ahlenstiel G, Shin EC, Herkel J, et al. Identification of CD4 T-cell epitopes in soluble liver antigen/liver pancreas autoantigen in autoimmune hepatitis. *Gastroenterology*. 2008;135:2107–18.
- Taubert R, Hardtke-Wolenski M, Noyan F, Wilms A, Baumann AK, Schlue J, et al. Intrahepatic regulatory T cells in autoimmune hepatitis are associated with treatment response and depleted with current therapies. *J Hepatol*. 2014;61:1106–14.
- Taylor SA, Assis DN, Mack CL. The contribution of B cells in autoimmune liver diseases. *Semin Liver Dis*. 2019;39:422–31.
- Muratori L, Parola M, Ripalti A, Robino G, Muratori P, Bellomo G, et al. Liver/kidney microsomal antibody type 1 targets CYP2D6 on hepatocyte plasma membrane. *Gut*. 2000;46:553–61.

25. Burak KW, Swain MG, Santodomingo-Garzon T, Lee SS, Urbanski SJ, Aspinall AI, et al. Rituximab for the treatment of patients with autoimmune hepatitis who are refractory or intolerant to standard therapy. *Can J Gastroenterol*. 2013;27:273–80.
26. Than NN, Hodson J, Schmidt-Martin D, Taubert R, Wawman RE, Botter M, et al. Efficacy of rituximab in difficult-to-manage autoimmune hepatitis: results from the international autoimmune hepatitis group. *JHEP Rep*. 2019;1:437–45.
27. Béland K, Marceau G, Labardy A, Bourbonnais S, Alvarez F. Depletion of B cells induces remission of autoimmune hepatitis in mice through reduced antigen presentation and help to T cells. *Hepatology*. 2015;62:1511–23.
28. Buitrago-Molina LE, Dywicki J, Noyan F, Schepergerdes L, Pietrek J, Lieber M, et al. Anti-CD20 therapy alters the protein signature in experimental murine AIH, but not exclusively towards regeneration. *Cell*. 2021;10:1471.
29. Liu X, Jiang X, Liu R, Wang L, Qian T, Zheng Y, et al. B cells expressing CD11b effectively inhibit CD4+ T-cell responses and ameliorate experimental autoimmune hepatitis in mice. *Hepatology*. 2015;62:1563–75.
30. Xiao S, Bod L, Pochet N, Kota SB, Hu D, Madi A, et al. Checkpoint receptor TIGIT expressed on Tim-1+ B cells regulates tissue inflammation. *Cell Rep*. 2020;32:107892.
31. Schultheiß C, Simnica D, Willscher E, Oberle A, Fanchi L, Bonzanni N, et al. Next-generation immunosequencing reveals pathological T-cell architecture in autoimmune hepatitis. *Hepatology*. 2021;73:1436–48.
32. Preti M, Schlott L, Lübbering D, Krzikalla D, Müller AL, Schuran FA, et al. Failure of thymic deletion and instability of autoreactive Tregs drive autoimmunity in immune-privileged liver. *JCI Insight*. 2021;6:e141462.
33. Neubert K, Meister S, Moser K, Weisel F, Maseda D, Amann K, et al. The proteasome inhibitor bortezomib depletes plasma cells and protects mice with lupus-like disease from nephritis. *Nat Med*. 2008;14:748–55.
34. Khodadadi L, Cheng Q, Alexander T, Sercan-Alp Ö, Klotsche J, Radbruch A, et al. Bortezomib plus continuous B cell depletion results in sustained plasma cell depletion and amelioration of lupus nephritis in NZB/W F1 mice. *PLoS One*. 2015;10:e0135081.
35. Matsushita T, Kobayashi T, Mizumaki K, Kano M, Sawada T, Tennichi M, et al. BAFF inhibition attenuates fibrosis in scleroderma by modulating the regulatory and effector B cell balance. *Sci Adv*. 2018;4:eaas9944.
36. Ishak K, Baptista A, Bianchi L, Callea F, De Groote J, Gudat F, et al. Histological grading and staging of chronic hepatitis. *J Hepatol*. 1995;22:696–9.
37. Schindelin J, Arganda-Carreras I, Frise E, Kaynig V, Longair M, Pietzsch T, et al. Fiji: an open-source platform for biological-image analysis. *Nat Methods*. 2012;9:676–82.
38. Bolotin DA, Poslavsky S, Mitrophanov I, Shugay M, Mamedov IZ, Putintseva EV, et al. MiXCR: software for comprehensive adaptive immunity profiling. *Nat Methods*. 2015;12:380–1.
39. Lee DW, Khavrutskii IV, Wallqvist A, Bavari S, Cooper CL, Chaudhury S. BRILIA: integrated tool for high-throughput annotation and lineage tree assembly of B-cell repertoires. *Front Immunol*. 2017;7:681.
40. Csardi G, Nepusz T. The Igraph software package for complex network research. *Int J Complex Syst*. 2006;1695.
41. Ma L, Qin J, Ji H, Zhao P, Jiang Y. Tfh and plasma cells are correlated with hypergammaglobulinaemia in patients with autoimmune hepatitis. *Liver Int*. 2014;34:405–15.
42. Abe K, Takahashi A, Imaizumi H, Hayashi M, Okai K, Kanno Y, et al. Interleukin-21 plays a critical role in the pathogenesis and severity of type I autoimmune hepatitis. *Springerplus*. 2016;5:777.
43. Fan X, Men R, Huang C, Shen M, Wang T, Ghnewa Y, et al. Critical roles of conventional dendritic cells in autoimmune hepatitis via autophagy regulation. *Cell Death Dis*. 2020;11:23.
44. Müller AL, Casar C, Preti M, Krzikalla D, Gottwick C, Averbhoff P, et al. Inflammatory type 2 conventional dendritic cells contribute to murine and human cholangitis. *J Hepatol*. 2022;77:1532–44.
45. Bouaziz JD, Yanaba K, Venturi GM, Wang Y, Tisch RM, Poe JC, et al. Therapeutic B cell depletion impairs adaptive and autoreactive CD4+ T cell activation in mice. *Proc Natl Acad Sci USA*. 2007;104:20878–83.
46. Lee DSW, Rojas OL, Gommerman JL. B cell depletion therapies in autoimmune disease: advances and mechanistic insights. *Nat Rev Drug Discov*. 2021;20:179–99.
47. Wilbrink R, Spoorenberg A, Verstappen GMPJ, Kroese FGM. B cell involvement in the pathogenesis of ankylosing spondylitis. *Int J Mol Sci*. 2021;22:13325.

SUPPORTING INFORMATION

Additional supporting information can be found online in the Supporting Information section at the end of this article.

How to cite this article: Lübbering D, Preti M, Schlott L, Schultheiß C, Weidemann S, Lohse AW, et al. Autoantigen-selected B cells are bystanders in spontaneous T cell-driven experimental autoimmune hepatitis. *Immunology*. 2023;170(2): 214–29. <https://doi.org/10.1111/imm.13665>